*Int. J. Electrochem. Sci.*, 8 **(2013)** 8371 - 8387

International Journal of
ELECTROCHEMICAL
SCIENCE
www.electrochemsci.org

# Electrochemical Study and Biological Activity of AZ91E Alloy in Hank's solution

*Wafaa M.Hosny and M. A.Ameer*[*]

Chemistry Department, Faculty of Science, Cairo University, Giza-12613, Egypt.
[*]E-mail: mameer_eg@yahoo.com,

*Received:* 21 March 2013 / *Accepted:* 30 April 2013 / *Published:* 1 June 2013

The electrochemical behavior of AZ91E alloy was investigated in Hank's solution at 37°C. The behavior of the alloy was studied with immersion time by using electrochemical impedance spectroscopy (EIS) and potentiodynamic tests. Also, the effect of adding different concentrations of a commercial drug, known as salicylhydroxamic acid (Sham), as inhibitor, in Hank's solution was studied. The corrosion was inhibited by addition of salicylhydroxamic acid that reacts with AZ91E alloy and forms a protective film on the surface at different concentration (0.01-1mM). The results were confirmed by surface examination via scanning electron microscope. The stability constant values of the binarycomplexes between salicylhydroxamic acid and metal ions Mg(II), Al(III) and Zn(II) formed in solution were investigated potentiometrically. The antimicrobial activity of these complexes has been screened against two *Gram-positive* and two *Gram-negative* bacteria and other bacteria. Antifungal activity against two different fungi has been evaluated and compared with reference drug.

**Keywords:** AZ91E alloy; EIS; potentiodynamic; SEM; Hank's solution; biological activity.

## 1. INTRODUCTION

The development of biodegradable implants is one of the most important research areas in medical science [1-3]. Since Mg alloys can gradually be dissolved and absorbed after implanting, it has been recently regarded as a potential biodegradable implant material due to its low density, high strength/weight ratio and similar elastic modulus to that of human bone (40–57 GPa) [4,5]. Mg or its alloys are non-toxic to the human body. Mg deficiency has been found to exacerbate the risk of hypertension, cardiac arrhythmias and osteoporosis, etc. [6]. There is growing evidence that if the releasing of Mg2+is acceptable by human body, it will help to stimulate the healing of bone tissue [7-9]. Moreover, magnesium has a high negative standard electrode potential (−2.37 V at 25 °C) and thus

is corroded relatively faster than other metallic materials, especially in $Cl^-$ containing aqueous environment, indicating that magnesium can degrade/or be corroded in a human body environment. Thus interface problems such as interface loosening and inflammation can be resolved and the second removal surgical operation for the case of bone screws and plates can be avoided. Thus, Mg alloy can gradually be dissolved and adsorbed after implanting [10-13]. A suitable degradation rate is critical to a biodegradable Mg implant before the tissue has been sufficiently recovered or healed [14]. After the recovery or healing, the implant should be gradually dissolved, consumed or absorbed by the human body. In fact, with recent developments and understandings of corrosion and prevention of Mg alloy, controlling the corrosion performance of Mg alloy should be possible now [15,16]. Extruded Mg alloy as AZ91E is getting more and more widely used because of its considerably high plasticity in comparison with the die-cast Mg alloys [17]. Several studies [18-20] have shown that the corrosion behavior of Mg alloys is significantly dependent on the alloying elements and the microstructure. Salicylhydroxamic acid is a drug that is a potent and irreversible inhibitor of bacterial and plant urease usually used for urinary tract infections. The molecule is similar to urea but is not hydrolysable by the urease enzyme [21]. It is also a trypanocidal agent. When administered orally, it is metabolized to salicylamide which exerts analgesic, antipyretic and anti-inflammatory effects. Salicylhydroxamic acid is also a common ligand utilized in the synthesis of metallacrowns. Hydroxamic acids have been used as therapeutic agents in chelating therapy and as metalloenzyme inhibitors [22-24]. Other medical applications of the hydroxamates which utilize their affinity for high charge density metal ions include the possible use of their metal complexes as imaging agents [25]. Quite recently, there have been articles concerning the biochemistry of anticancer activity of naturally occurring and synthetic class of organic compounds containing the hydroxamic acid functional group (-CONHOH). Hydroxyurea containing that group is a well known anticancer drug [26-29]. It inhibits the DNA synthesis by impairing the activity of enzyme ribonucleotide reductase [28-31]. The rate of O2 uptake by *C. albicans* is inhibited [32] by salicylhydroxamic acid or KCN. Simple hydroxamate analogues (salicylhydroxamic acids) (Scheme 1) can undergo two deprotonation processes and act as bidentate ligands [33,34].

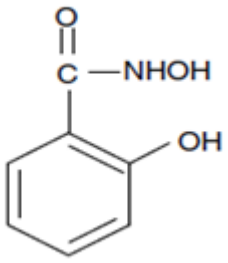


**Scheme 1.** Salicylhydroxamic acids

The hydroxamates are of interest due to their ability to form stable transition metal complexes through the formation of a five membered chelate ring as shown in Scheme 2 [35]. In this investigation, we report a quantitative study of the acid base equilibrium of Salicylhydroxamic acid, as

well as the binary complex formation equilibria with Mg(II), Al(III) and Zn(II). Such work may help to explain the nature and driving forces for the interactions occurring in biological systems, such as metal-protein and metal-nucleic acid interactions.

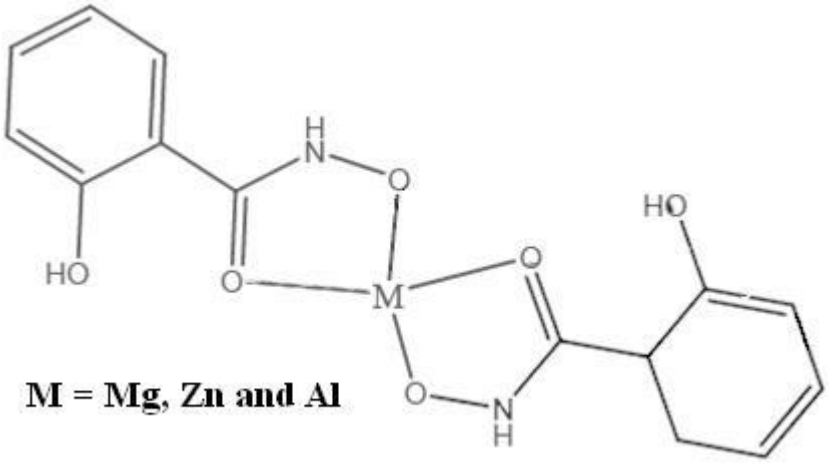


**Scheme 2.** The chemical structures of salicylhydroxamic acid complex

In plants, some fungi and some protests with the alternative oxidase (AOX) enzyme in the mitochondrial electron transport chain system, salicylhdroxamic acid acts as an inhibitor of the enzyme, blocking the largely uninhibited flow of electrons through AOX [36]. The present study aims to investigate the influence of Hank's solution on the dissolution and passivation features of magnesium-based AZ91E alloy (biodegradable materials for temporary implant) with immersion time at 37°C. Furthermore, the feasibility to slow down the biodegradation (i.e. corrosion) of magnesium alloys to solve the rapidly corroding magnesium implant problems was demonstrated by studying the effect of adding Salicylhydroxamic acid to Hank's solution on the corrosion behavior of AZ91 alloy using electrochemical ( impedance and polarization) techniques .Also the biological activity of the tested solution was discussed.

## 2. EXPERIMENTAL

An extruded magnesium aluminum alloy ( AZ91E) donated from Department of mining, Metallurgy and Materials Engineering, Laval University, Canada with chemical composition (wt%): 9.0 Al, 0.7 Zn, 0.13 Mn, 0.03 Cu, 0.01 Si, 0.006 Fe,0.004 Ni, 0.0007 Be and balance Mg. The sample was divided into small coupons. Each coupon was welded to an electrical wire and fixed with Araldite epoxy resin in a glass tube leaving cross-sectional area of the specimen 0.196 $cm^2$ for both AZ91E alloy. The solution used was Hank's balanced salt solution with composition (g/l): NaCl 8.00, $NaHCO_3$ 0.35, $Na_2HPO_4$ 0.0477, $KH_2PO_4$ 0.06, KCl 0.40, and D-Glucose 1.0. The pH of the solution was 7.4. Salicylhydroxamic acid was provided from Nasr pharmaceutical chemical company, Egypt. The metal salts used are $MgCl_2.6H_2O$, $AlCl_3.6H_2O$ and $ZnCl_2$, obtained from Sigma Chem. Co, UK. Metal salt

solutions were prepared and standardized as described previously [37]. Salicylhydroxamic acid and Hank's solution reagents are Analar and solutions are prepared using triply distilled water. The surface of the test electrode was mechanically polished by emery papers with 400 up to 1000 grit to ensure the same surface roughness, degreasing in acetone, rinsing with ethanol and drying in air. The cell used was a typical three-electrode one fitted with a large platinum sheet of size 15×20×2 mm as a counter electrode (CE), saturated calomel (SCE) as a reference electrode (RE) and the alloy as the working electrode (WE). The impedance diagrams were recorded at the free immersion potential (OCP) by applying a 10 mV sinusoidal potential through a frequency domain from 3 kHz down to 100 mHz. The instrument used is the electrochemical workstation IM6e Zahner-elektrik, GmbH, (Kronach, Germany).The electrochemical experiments were always carried inside an air thermostat which was kept at 37°C, unless otherwise stated. The SEM micrographs were collected using a JEOL JXA-840A electron probe microanalyzer. Antimicrobial activity of the tested samples was determined using a modified Kirby–Bauer disc diffusion method [38]. The antibacterial activities were done by using gram +ve organisms (Staphylococcus aureus and Bacillus subtillis) and gram –ve organisms (Escherichia coli and Pseudomonas aeruginosa). These bacterial strains were chosen as they are known human pathogens. Briefly,100 µl of the test bacteria were grown in 10 ml of fresh media until they reached a count of approximately 108 cells/ml or 105 cells/ml for fungi [39]. Hundred microliters of microbial suspension was spread onto agar plates corresponding to the broth in which they were maintained. Isolated colonies of each organism that might be playing a pathogenic role should be selected from primary agar plates and tested for susceptibility by disc diffusion method of the National Committee for Clinical Laboratory Standards (NCCLS) [40]. Among the available media available, NCCLS recommends Muller6 Hinton agar due to: it results in good batch-to-batch reproducibility. Plates inoculated with Gram (+) bacteria as S. aureus, B. subtilis; Gram (-) bacteria as E. coli, P.aeuroginosa, they were incubated at 35–37 °C for 24–48 h and fungi as Aspergillus flavus and Candida albicans incubated at 300 C for 24–48 h and then the diameters of inhibition zones were measured in millimeters[38]. Standard discs of Ampicillin (Antibacterial agent), Amphotericin B (Antifungal agent) served as positive controls for antimicrobial activity but filter discs impregnated with 10 µl of solvent were used as a negative control. The solution in different concentrations (mg/ml) of each compound (free ligand, metal complexes and standard drug) in DMSO was prepared for testing against spore germination. The agar used is Muller-Hinton agar that is rigorously tested for composition and pH. Further the depth of the agar in the plate is a factor to be considered in the disc diffusion method. This method is well documented and standard zones of inhibition have been determined for susceptible and resistant values. When a filter paper disc impregnated with a tested chemical is placed on agar, the chemical will diffuse from the disc into the agar. This diffusion will place the chemical in the agar only around the disc. The solubility of the chemical and its molecular size will determine the size of the area of chemical infiltration around the disc. If an organism is placed on the agar, it will not grow in the area around the disc if it is susceptible to the chemical. This area of no growth around the disc is known as a ‘‘Zone of inhibition’’ or ‘‘Clear Zone’’. For the disc diffusion, the zone diameters were measured with slipping calipers of the (NCCLS) [40]. Agar based methods such as E-test and disk diffusion can be good alternatives because they are simpler and faster the broth-based methods [41,42]. Potentiometric measurements were made using a Metrohm 751

Titrino. The titroprosessor and electrode were calibrated with standard buffer solutions, prepared according to NBS specifications [37] at 25 ± 0.1°C and I = 0.1 mol $dm^{-3}$, potassium hydrogen phthalate (pH 4.008) and a mixture of $KH_2PO_4$ and $Na_2HPO_4$ (pH 6.865). (0.10 mol $dm^{-3}$) standard acid solution was titrated with a standard base (0.10 mol $dm^{-3}$) to convert the pH meter reading into hydrogen ion concentration. The pH values was plotted against p[H], where the relation pH- p[H] =0.5 was observed for all the titration data. A pKw value of 13.997[43] was used to calculate the [$OH^-$]. The titrations were performed in a thermostated titration vessel equipped with a magnetic stirring system, under purified $N_2$ atmosphere using 0.05 M NaOH as titrant. The titrations were performed at a constant ionic strength of 0.1 mol $dm^{-3}$ ($NaNO_3$). The acid dissociation constants of the ligand were determined by titrating a 40 ml of ligand solution ($1.25\times10^{-3}$ mol $dm^{-3}$). The formation constants of the complexes were determined by titrating 40 ml of the solution containing metal ion ($1.25\times10^{-4}$mol $dm^{-3}$) and ligand ($1.25\times10^{-3}$ mol $dm^{-3}$). The stability constant values were calculated by using the computer program MINIQUAD-75[44]. Various possible composition models were tried to calculate the stoichiometry and stability constants of the system studied. The model selected was that which gave the best statistical fit as described before [44]. The experimental titration data points were compared with the theoretical curve calculated from the acid dissociation constant values of the ligand and the formation constants of their complexes, in order to check the validity of the selected model. The speciation diagrams were obtained using the program SPECIES [45]. UV-Vis spectrophotometric measurements were carried out using automated spectrophotometer UV-Vis Thermo Fischer Scientific Model Evolution 60 ranged from 200 to 900 nm.

## 3. RESULTS AND DISCUSSION

### *3.1. EIS measurements*

#### *3.1.1. Effect of Salicylhydroxamic acid concentration*

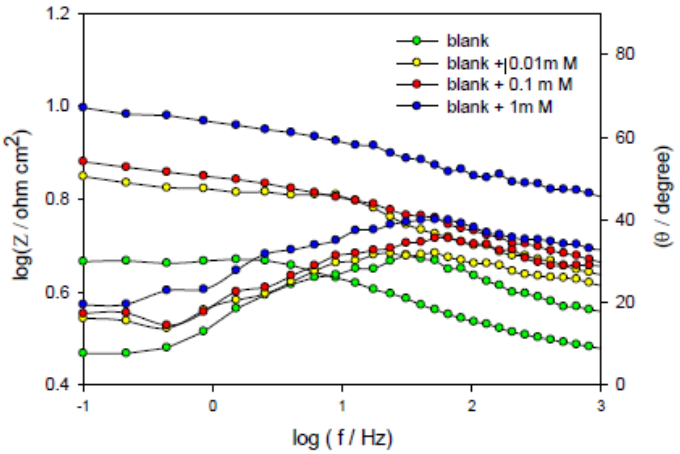


**Figure 1.** Bode plots for AZ91E alloy in Hank's solution (blank) without and with different concentration of salicylhydroxamic acid at 37°C.

Electrochemical impedance (EIS) is a technique with small perturbative signal and the surface damage of the sample is very little. Besides, the corrosion mechanism can be estimated by analyzing the measured electrochemical impedance spectrum. Salicylhydroxamic acid is a trypanocidal agent. When administered orally, it is metabolized to salicylamide which exerts analgesic, antipyretic and anti-inflammatory effects. Thus, it is intended in this part to study the effect of adding Salicylhydroxamic acid to Hank's solution on the electrochemical behavior of the biodegrable AZ91 alloy. Fig 1.shows EIS results probed after 2h immersion in Hank's solution in absence and presence of various concentrations of salicylhydroxamic acid in the range from 0.01 to 1 mM, and presented as Bode plots. The general feature of the plots suggests that the presence of Salicylhydroxamic acid in the solution do not alter the reaction responsible for corrosion. The Bode format confirms the presence of two time constants as there are two maximum phase lags appears at medium frequencies (MF), and low frequencies (LF).

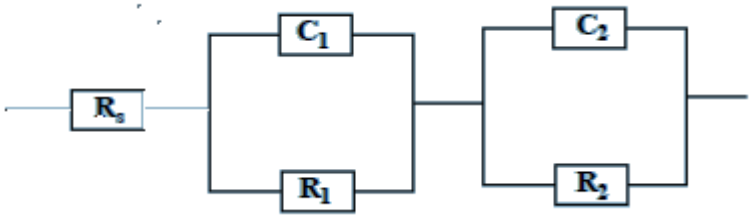


**Figure 2.** The equivalent circuit model

On the other hand, for the impedance diagrams with two time constants the appropriate equivalent model, shown in Fig. 2, consists of two circuits in series from $R_1C_1$ and $R_2C_2$ parallel combination and the two are in series with $R_s$. In this way $C_1$ is related to contribution from the capacitance of the outer layer and the faradic reaction therein and $C_2$ pertains to the inner layer, while $R_1$ and $R_2$ are the respective resistances of the outer and inner layers constituting the surface film, respectively [46,47]. Analysis of the experimental spectra was made by best fitting to the corresponding equivalent circuit using Thales software provided with the workstation where the dispersion formula suitable to each model was used [48]. In this complex formula an empirical exponent (α) varying between 0 and 1, is introduced to account for the deviation from the ideal capacitive behaviour due to surface inhomogenities, roughness factors and adsorption effects [48]. In all cases, good conformity between theoretical and experimental was obtained for the whole frequency range. For this model the electrode impedance is represented by the following transfer function [49-51]:

$$Z(\omega)=R_o+\frac{R_1}{1+R_1C_1(j\omega)^{\alpha_1}}+\frac{R_2}{1+R_1C_1(j\omega)^{\alpha_2}} \qquad (1)$$

The above formula takes into account the deviation from the ideal RC behavior and considers, for a more realistic approach that each oxide layer as non-homogeneous. Thereby, the impedance associated with the capacitance of each layer is described by a constant phase element (CPE).

*3.1.2. Effect of immersion time*

In these experiments, the immersion of magnesium alloy was carried out continuously in Hank's solution which is used to simulate the biochemical reaction of the magnesium alloy in human physiological conditions.

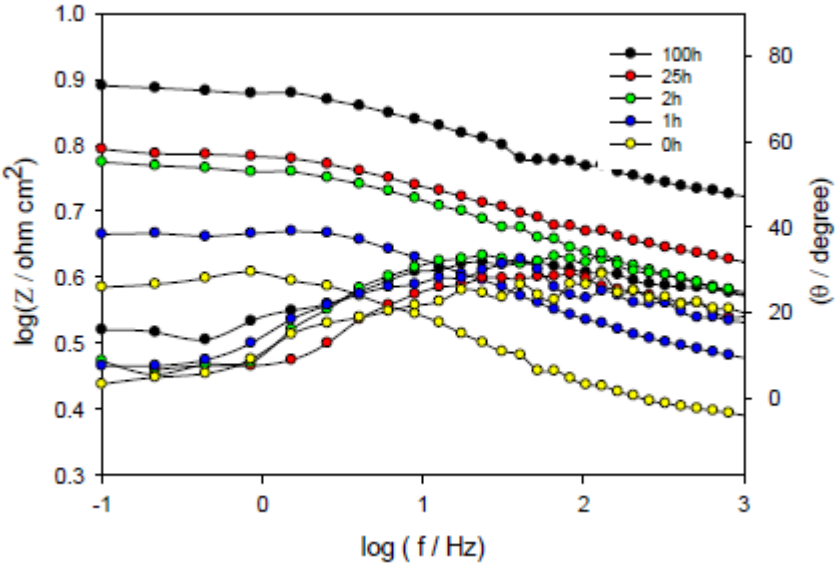


**Figure 3.** Bode plots for AZ91E alloy in Hank's solution (blank) at different immersion time.

The specimens were suspended in Hank's solution up to 100 hour. The EIS scans as Bode plots at different immersion times are given in Fig.3 for AZ91 alloy. It can be seen that these diagrams show resistive regions at high and low frequencies and capacitive contribution at intermediate frequencies. The impedance ($|Z|$) as well as the phase shift θ for the alloy is clearly found to depend on immersion time. It is observed that an increase in time of immersion, from 0 to 100 h (Fig. 3), continuously decreases the $|Z|$ and θ values.

**Table 1.** Impedance Parameters of AZ91E alloy in Hank's solution at 37°C.

| Time hour | Rs/ Ω cm$^2$ | $R_1$ / Ω cm$^2$ | $C_1$ / μF cm$^{-2}$ | $\alpha_1$ | $R_2$ / Ω cm$^2$ | $C_2$ / μF cm$^{-2}$ | $\alpha_2$ |
|---|---|---|---|---|---|---|---|
| 0 | 3.60 | 2.04 | 140.8 | 0.75 | 10.5 | 40.3 | 0.71 |
| 1 | 2.82 | 2.47 | 112.0 | 0.78 | 12.0 | 25.5 | 0.72 |
| 2 | 2.27 | 2.64 | 107.1 | 0.75 | 12.8 | 22.1 | 0.72 |
| 25 | 3.67 | 2.99 | 95.5 | 0.76 | 17.7 | 20.5 | 0.75 |
| 100 | 2.03 | 3.85 | 75.7 | 0.79 | 50.1 | 11.0 | 0.74 |

This trend is most likely a result of a decrease in the surface film resistance commensurate with a decrease in the adsorbed amount of anions forming Hank's solution as $Cl^{-l}$, $HCO_3^-$, $H_2PO_4^-$ or $HPO_4^{-2}$ on the electrode surface [46].The Bode format of Fig. 3 confirms the presence of two time constants as there are two maximum phase lags appears at medium frequencies (MF), and low frequencies (LF). On the other hand, for the impedance diagrams with two time constants the appropriate equivalent model, shown in Fig. 2, consists of two circuits in series from $R_1C_1$ and $R_2C_2$ parallel combination and the two are in series with $R_s$. The experimental values are correlated to the theoretical impedance parameters of the equivalent model and listed in Tables 2 for AZ91E alloy in Hank's solution.

As given in Tables 1, it was found that film healing and thickening becomes effective by increasing time of immersion in Hank's solution leading to a quasi-steady state thickness at longer times. This is caused by the formation of adherent corrosion products on the sample surface including, magnesium hydroxide, as well as phosphates and carbonates [52]. They are precipitated from the solution during the corrosion of magnesium alloys due to saturation and localized alkalization [53]. Metal ions released from corrodible alloys to the surrounding tissues may cause biological responses in short term or prolonged periods. The toxicity of a metallic material is governed not only by its composition and toxicity of the component elements but also by its corrosion and wear resistance [53].

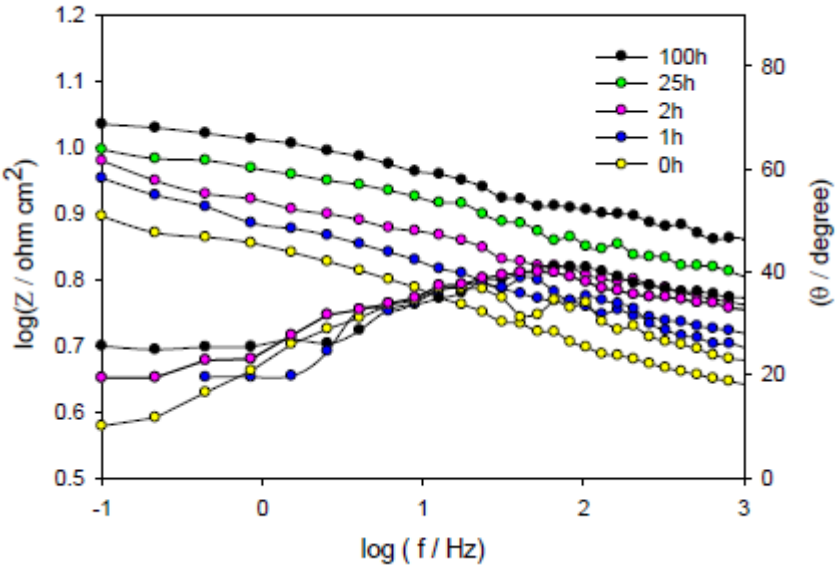


**Figure 4**. Bode plots for AZ91E alloy in Hank's solution (blank) containing 1 mM salicylhydroxamic acid at different immersion time.

In a saline environment, magnesium-based alloys would be degraded to magnesium chloride, oxide, sulphate or phosphate [54] and the same occur in Hank's solution. Also, magnesium carbonate precipitated on the surface of magnesium alloy improved the corrosion resistance of magnesium alloy in the case of atmospheric corrosion [55]. For chloride ions, in poorly buffered chloride solutions, they reveal low corrosion rates due to the formation of a partially protective Mg $(OH)_2$ layer. Also, phosphates inhibit dissolution of the oxide film with increasing immersion time [56]. Phosphate is

formed on the oxide surface and prevents dissolution. Generally, Hank's solution improves slightly the corrosion resistance of AZ91E alloys with time. It should be noted that the alloying elements Al and Zn tend to have a stabilizing effect on the protective film formed on an Mg alloy. Indeed, without these alloying elements, pure magnesium experiences a much faster biodegradation under similar testing conditions [57]. It was reported that the content of Al in the second phase particles might be the $\beta$ phase ($Mg_{17}$ $Al_{12}$), the electrode potential of the $\beta$ phase is higher than the matrix; therefore, it will form microcells with the adjacent matrix and accelerate the corrosion process[58].

The electrochemical behavior of the biodegradable AZ91 alloy on adding 1 mM salicylhydroxamic acid to Hank's solution on was studied. Fig. 4.shows EIS results probed after 100h immersion in Hank's solution in presence of 1 mM, and presented as Bode plots (Table 2). In all solutions the impedance, |Z| value decrease with increasing added salicylhydroxamic acid concentration, however the 1 mM shows a critical concentration which has higher resistance compared to that of 0.1 and 0.01 mM salicylhydroxamic acid solution. However, 0.1 mM salicylhydroxamic acid concentration is much better than 0.01mM concentration.

**Table 2.** Impedance Parameters of AZ91E alloy in Hank's solution with 1mM salicylhydroxamic acid at 37°C.

| Time hour | Rs/ $\Omega$ cm$^2$ | $R_1$ / $\Omega$ cm$^2$ | $C_1$ / $\mu$F cm$^{-2}$ | $\alpha_1$ | $R_2$ / $\Omega$ cm$^2$ | $C_2$ / $\mu$F cm$^{-2}$ | $\alpha_2$ |
|---|---|---|---|---|---|---|---|
| 0 | 2.60 | 3.64 | 130.8 | 0.75 | 12.5 | 30.3 | 0.77 |
| 1 | 3.82 | 4.07 | 102.0 | 0.79 | 14.0 | 15.5 | 0.76 |
| 2 | 2.27 | 4.24 | 97.1 | 0.75 | 14.8 | 12.1 | 0.72 |
| 25 | 3.23 | 4.59 | 75.5 | 0.78 | 27.7 | 10.5 | 0.75 |
| 100 | 2.07 | 5.55 | 55.7 | 0.79 | 60.1 | 7.7 | 0.74 |

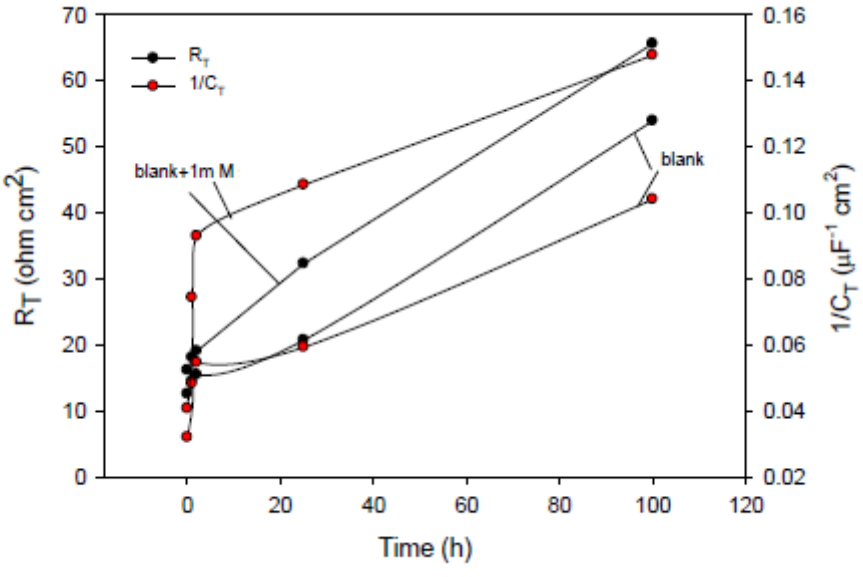


**Figure 5.** $R_T$ and $1/C_T$ as a function of immersion time for AZ91E alloy in blank solution without and with 1mM of Salicylhydroxamic acid at 37°C

The total resistance ($R_T$) and the relative thickness ($1/C_T$) for AZ91 alloy in Hank's solution in absence and presence of 1 mM salicylhydroxamic acid solutions as a function of the immersion time are presented in Fig.5. The impedance data were simulated to the equivalent circuit represented in Fig. 2. Both values increase with immersion time. Also, the total resistance $R_T$ and the relative thickness $1/C_T$ of the film formed on the alloy show always higher values compared to the values in absence of salicylhydroxamic acid as illustrated in Fig.5.

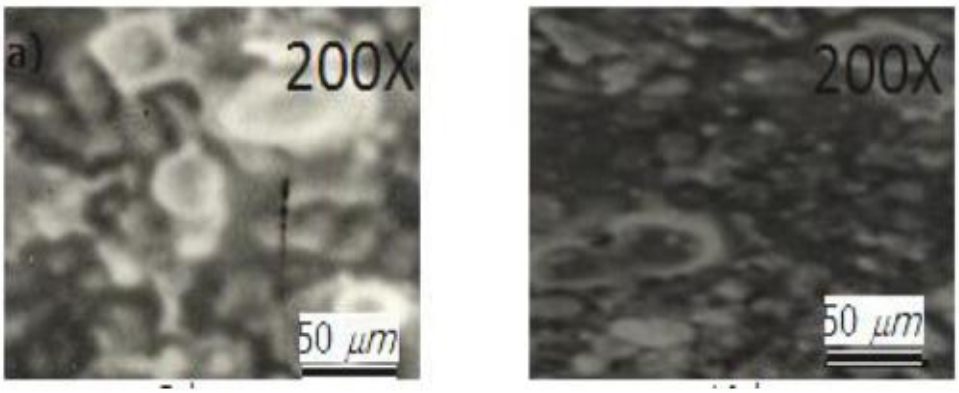


A B

**Figure 6**. SEM micrographs for AZ91E alloy after 100 h of immersion in blank solution without salicylhydroxamic acid (A) and (B) with 1 mM salicylhydroxamic acid.

This was confirmed by scanning electron microscope (SEM) images shown in Fig. 6A,B. Fig. 6B shows a smoother film adsorbed on the alloy surface for 1 mM than that in absence of salicylhydroxamic acid Fig. 6A.

*3.2. Potentiodynamic polarization measurements*

**Table 3.** Electrochemical Parameters of AZ91E alloy in Hank's solution without and with 1mM salicylhydroxamic acid at 37°C.

| Conc. (mol/l) | -Ecorr (V) | $i_{corr}$ ($A/cm^2$) | $-\beta c$ (mV/dec) | $\beta a$ (mV/dec) |
|---|---|---|---|---|
| Blank | 0.81 | 3.64 | $1.99x10^{-3}$ | 84 |
| $10^{-5}$ | 0.49 | 4.07 | $9.89x10^{-6}$ | 81 |
| $10^{-4}$ | 0.45 | 4.24 | $2.0x10^{-7}$ | 130 |
| $10^{-3}$ | 0.33 | 4.59 | $2.5x10^{-9}$ | 127 |

In these experiments, the potential was scanned from -1.5 to 0.5 V vs. SCE at a rate of 1 mV s-1, prior to the potential scan the electrode was left under open circuit conditions in the respective solution for 2 h until a steady free corrosion potential ($E_{st}$) value was recorded. Fig. 7 shows a typical

linear sweep potentiodynamic trace for the AZ91alloy in blank solution without and with different concentration of salicylhydroxamic acid (0.01-1mM). It is noticed that the corrosion potential shifts towards more anodic potential as the concentration increases as shown in Table 3. In the anodic range a current plateau is observed. The results in Table 4 indicate clearly that the corrosion current density ($i_{corr}$) is dependent on the salicylhydroxamic acid concentration.

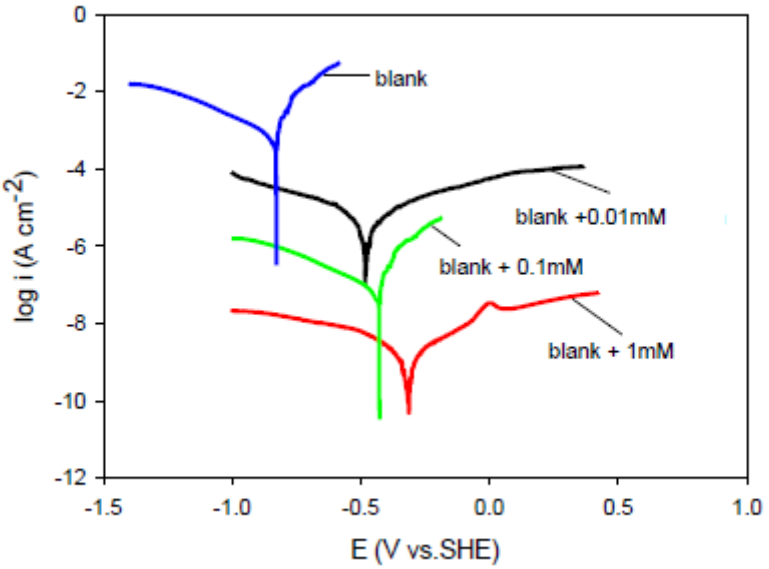


**Figure 7**. Potentiodynamic polarization curves for AZ91E in blank solution without(blank) and with different concentration of salicylhydroxamic acid at 37$^{o}$C.

**Table 4.** Stability constants of salicylhydroxamic acid complexes where ap, q and r are the stoichiometric coefficients corresponding to metal (II), Salicylhydroxamic acid and $H^{+}$ respectively. b standard deviation are given in parentheses. c sum of square of residuals

| System | p | q | r[a] | *log*$\beta^{b}$ | $S^{c}$ |
|---|---|---|---|---|---|
| Salicylhydroxamic acid | 0 | 1 | 1 | 9.85(0.01) | $5.10x10^{-7}$ |
| | 0 | 1 | 2 | 17.41(0.02) | |
| Mg- Salicylhydroxamic acid | 1 | 1 | 0 | 5.69(0.02) | $5.70x10^{-8}$ |
| | | | | 8.01(0.01) | |
| Al- Salicylhydroxamic acid | 1 | 1 | 0 | 12.34(0.03) | 4.2x10-8 |
| | 1 | 2 | 0 | 20.59(0.02) | |
| Zn- Salicylhydroxamic acid | 1 | 1 | 0 | 6.02(0.02) | $6.70x10^{-9}$ |
| | 1 | 2 | 0 | 10.08(0.04) | |

*3.3. Proton hydroxamic acid equilibria*

The protonation constants of the salicylhydroxamic acid used can be readily calculated from the titration data within the pH range 2- 11, whereby protonation equilibrium reactions have been found to be feasible. Salicylhydroxamic acid contains two hydroxyl groups, so that the potentiometric

titration curve (Fig. 8), shows two buffer regions.The first one extends up to the neutralization point of the hydroxamic proton, i.e. at a= 1 (a = moles of base added per mole of ligand). The second region lies within the 1≤ a ≥ 2 range, and is most likely associated with the neutralization of the phenolic hydroxyl group of salicylhydroxamic acid. The stepwise protonation constants amount to log $K^H$ = 9.68 ± 0.01 for the phenolic group and log $K^H$= 7.34±0.01 for the hydroxamic hydroxyl group, were obtained at 25°C and I=0.1 mol $dm^{-3}$ $NaNO_3$.

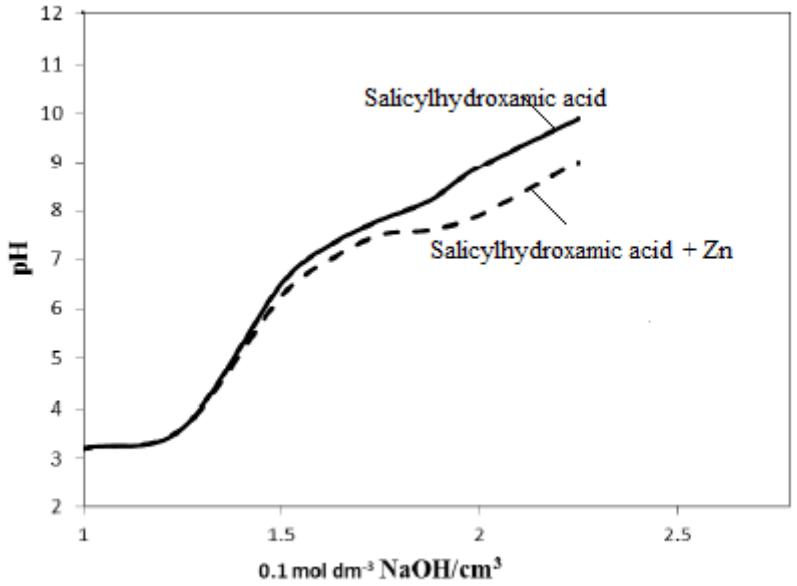


**Figure 8.** Potentiometric titration curves for salicylhydroxamic acid ($H_2L$) and $ZnL_2$ systems.

The greater acidity of the hydroxamic acid OH group in salicylhydroxamic acid relative to that of other acid analogue is due to stabilization of the conjugate base by intermolecular hydrogen bonding with the phenolic OH group. The results obtained are in good agreement with literature values [59-61].

*3.4. Binary complexes involving Salicylhydroxamic acid with the metal ions Mg(II), Al(III) and Zn(II)*

Table 4, lists the stoichiometry and stability constants of the binary complexes [62] formed with salicylhydroxamic acid together with the proton association constants of salicylhydroxamic acid. The metal ions with the ligand are titrated potentiometrically with NaOH. A displacement was observed in the metal-ligand titration curves compared to the ligand titration curve. This indicated the release of protons upon complex formation. The potentiometric titration data of the binary complex formation equilibria were fitted to various models.

The titration data fit satisfactory with the formation of the deprotonated species 110 (Metal: ligand 1:1), and the deprotonated species 120 (Metal: ligand 1:2). Al (III) form two types of complexes, 1:1 and 1:2, the former complex predominates at pH <3.0, while 1:2 formed at pH=4.0. As the complexes are formed at low pH, therefore it can be suggested that both may have high stability

constant, in case of Mg(II) and Zn(II) with salicylhydroxamic acid, there are very weak complexion between both metal ions and salicylhydroxamic acid compared to Al(III). Stability constants of salicylhydroxamic acid complexes where ap, q and r are the stoichiometric coefficients corresponding to metal (II), salicylhydroxamic acid and $H^+$ respectively. b standard deviation are given in parentheses. c sum of square of residuals Fig. 9, shows the UV-Vis absorption spectra of the binary complexes (2.5 x 10-4 M) in water. Two absorption peaks at 250 and 300 nm are observed in salicylhydroxamic acid with molar absorbance in range of (1.43–3.87)x105 L $mol^{-1}$ $cm^{-1}$; this may be due to $\pi - \pi^*$ and $n - \pi^*$ transition within the ligand [62].

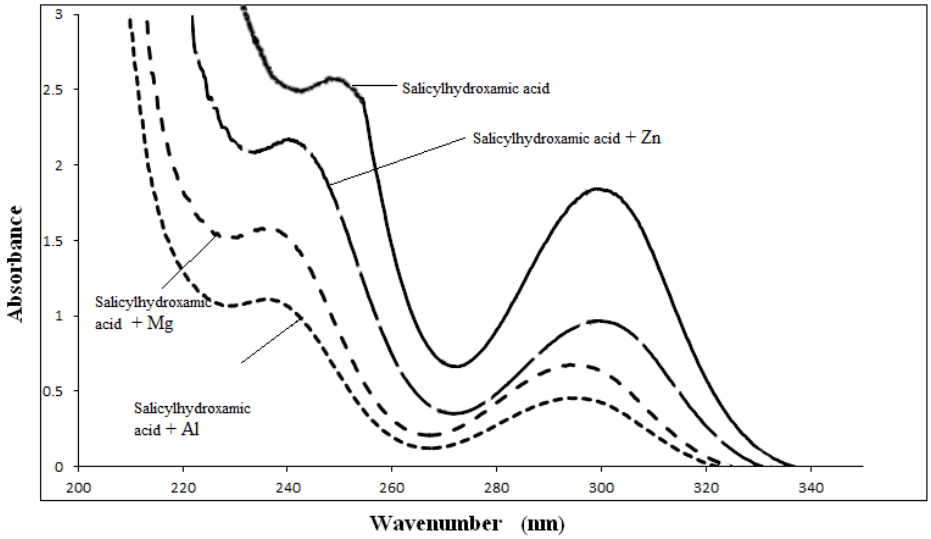


**Figure 9**. UV-Vis absorption spectra (2.5 x $10^{-4}$ M) of the title ligand and complexes

A relatively low bathochromic shift is observed in the binary complexes ($\Delta\lambda$ was in the range of 3–12 nm) and their molar absorbance was in the range of (1.102–3.918) x105 l $mol^{-1}$ $cm^{-1}$. The coordination of the metal ions through the phenolic and hydroxamic hydroxyl groups in salicylhydroxamic acid can be the reason for this red shift of the maximum absorption peaks.

### *3.5. Antimicrobial activity*

The salicylhydroxamic acid ligand is biologically active and its activity may arise from the hydroxamic group which may play an important role in the antibacterial activity [63]. To assess the biological potential of the synthesized compounds, the salicylhydroxamic acid ligand, its metal complexes and the emulsion electrolytic solution (blank+ 1mM salicylhydroxamic acid after 100 h immersion time) which exposed to air more than 10 hours which contained the corrosive zinc and magnesium metals were tested against the selected bacteria and fungi (Fig. 10). The antimicrobial data were collected in Table 5.

**Table 5.** Antibacterial activity of the isolated complexes

| S. No. | Compounds | Diameter of inhibition zone ( mm ) | | | | | | | |
|---|---|---|---|---|---|---|---|---|---|
| | | E. coli | P.aeuruginosa | S.aureus G- | S.aureus G+ | P.Vulgaris | E.cloacae | A. flavus | C.albicans |
| 1 | Salicylhydroxamic acid | 13 | 13 | 15 | 10 | 13 | 14 | 0 | - |
| 2 | Salicylhydroxamic acid + Zn | 25 | 22 | 21 | 17 | 19 | 20 | 0 | 12 |
| 3 | Salicylhydroxamic acid + Al | 22 | 20 | 20 | 16 | 19 | 19 | 0 | 11 |
| 4 | Salicylhydroxamic acid + Mg | 19 | 17 | 16 | 13 | 15 | 16 | 0 | 8 |
| 5 | Electrolytic solution | 9 | 10 | 12 | 6 | 4 | 3 | 0 | - |
| 6 | Tetracycline | 30 | 28 | 33 | 28 | 28 | 29 | - | - |
| 7 | Amphotericin B | - | - | - | - | - | - | 17 | 19 |

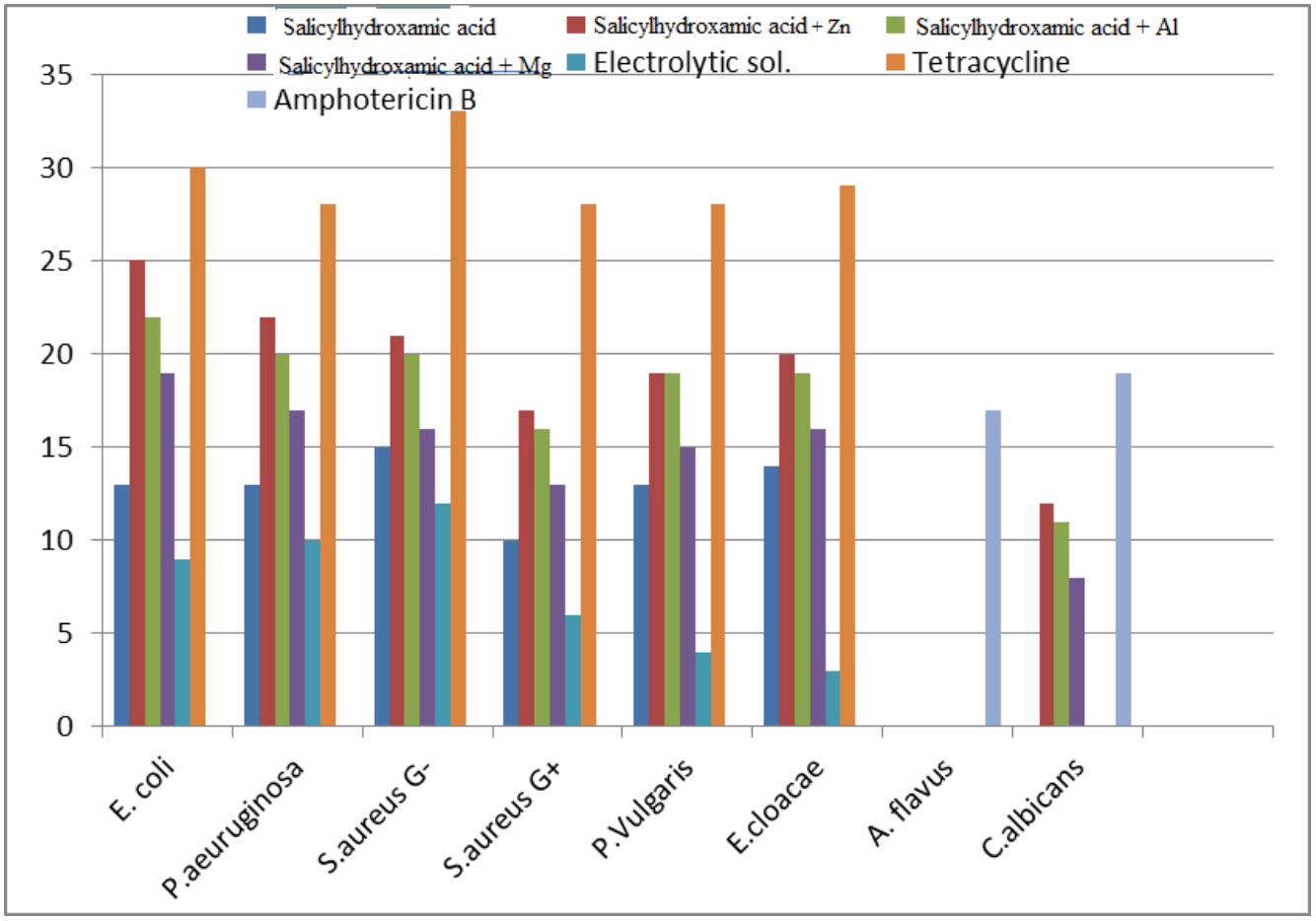


**Figure 10.** Biological activity of the tested samples against *S. aureus* (*G+*), *E .coli* (*G-*), *A. flavus*, *C. albicans.*

The synthesized compounds were found to be more toxic compared with their parent ligands against the same micro-organism and under the identical experimental conditions. The increase in biological activity of the metal chelates may be due to the effect of the metal ion on the normal cell process. A possible mode of toxicity increase may be considered in the light of Tweedy's chelating

theory [64]. Chelating considerably reduce the polarity of the metal ion because of partial sharing of its positive charge with the donor group and possible p-electron delocalization within the whole chelate ring system that is formed during coordination. Such chelating could enhance the lipophilic character of the central metal atom and hence increasing the hydrophobic character and lipo solubility of the complex favoring its permeation through the lipid layers of the cell membrane. This enhances the rate of uptake/entrance and thus the antimicrobial activity of the testing compounds. Accordingly, the antimicrobial activity of the three complexes can be referred to the increase of their lipophilic character which in turn deactivates enzymes responsible for respiration processes and probably other cellular enzymes, which play a vital role in various metabolic pathways of the tested microorganisms. The antibacterial activity can be ordered as:

[Zn(Salicylhydroxamic acid)] > [Al(Salicylhydroxamic acid)] > [Mg(Salicylhydroxamic acid)], suggesting that the lipophilic behavior increases in the same order. The results indicate that, the two complexes exhibited moderate activity against the fungal strains when compared with standard Amphotericin. The tested complexes were more active against Gram-positive than Gram-negative bacteria, it may be concluded that the antimicrobial activity of the compounds is related to cell wall structure of the bacteria. It is possible because the cell wall is essential to the survival of bacteria and some antibiotics are able to kill bacteria by inhibiting a step in the synthesis of peptidoglycan. Gram-positive bacteria possess a thick cell wall containing many layers of peptidoglycan and teichoic acids,but in contrast, Gram negative bacteria have a relatively thin cell wall consisting of a few layers of peptidoglycan surrounded by a second lipid membrane containing lipopolysaccharides and lipoproteins. These differences in cell wall structure can produce differences in antibacterial susceptibility and some antibiotics can kill only Gram-positive bacteria and is infective against Gram-negative pathogens [65]. Structure activity relationships indicate that the complexation with aluminum, zinc and magnesium enhances the antimicrobial activity of the ligands against some of the tested organisms. Since zinc and aluminum chelates have an enhanced antimicrobial activity, in comparison to their analogous containing magnesium (II) ions, the metal seems to play a relevant role in the activity of these compounds. These results may be due to higher stability constant of the Al (III) and Zn(II) complexes compare to Mg(II) complex (Table 5).

## 4. CONCLUSIONS

- The corrosion resistance of AZ91E alloy increases with immersion time in Hank's solution.
- The total resistance $R_T$ and the relative thickness $1/C_T$ of the film formed on AZ91E alloy show always higher values compared to that in absence of salicylhydroxamic acid.
- The inhibition of AZ91E alloy by salicylhydroxamic acid follows the order: Blank <Blank + 0.01 mM Salicylhydroxamic acid <Blank + 0. 1 mM Salicylhydroxamic acid <Blank + 1 mM Salicylhydroxamic acid and this was confirmed by SEM images.
- The potentiometric titration data showed The results showed that the stability

of the complexes can be ordered as:

Mg (Salicylhydroxamic acid) < Zn (Salicylhydroxamic acid) < Al(Salicylhydroxamic acid).

- The antibacterial activity of the isolated metal chelates obeyed this order.

**References**


1. G. Mani, M. Feldman, D. Patel and M. Agrawal, *Biomat* ,28 (2007) 1689.
2. L. Nair and C.Laurencin, *Prog. Polym.Sci*., 32 (2007) 762.
3. 3.G. Song andS. Song, *Adv. Eng.Mater*., 4 (2007) 298.
4. F. Witte, H. Ulrich, M. Rudert and E. Willbold, *J. Biomed. Mater. Res*., A (2007) 748.
5. M.Staiger, A. Pietak, et al., *Biomat*., 27 (2006) 1728.
6. J. Vormann, *Mol. Aspects Med*., 24 (2003) 27.
7. F.Wolf and A. Cittadini, *Mol. Aspects Med*., 24 (2003) 3.
8. R.Rude, *J. Bone Miner. Res*., 13 (1998) 749.
9. R. Rude, *J. Nutr. Biochem*., 15 (2004) 710.
10. P.Revell, E. Damien, X. Zhang, P. Evans and C.Howlett, *Key Eng. Mater*.254 (2004) 447.
11. H. Zreiqat, C.R. Howlett, A. Zannettino, P. Evans,G.Schulze-Tanzil, C.Knabe and M.Shakibaei, *J. Biomed. Mater. Res*.,62 (2002) 175.
12. Y. Yamasaki, Y. Yoshida, M. Okazaki, A. Shimazu, T. Uchida, T. Kubo, et al., *J.Biomed. Mater. Res*., 62 (2002) 99.
13. Y. Yamasaki, Y. Yoshida, M. Okazaki, A. Shimazu, T. Kubo, Y. Akagawa, et al., *Biomat*., 24 (2003) 4913.
14. F. Witte, V. Kaese, H. Haferkamp, E. Switzer, et al., *Biomat*., 26 (2005) 3557.
15. G. Song and A. Atrens, *Adv. Eng. Mater*., 5 (2003) 837.
16. G. Song, *Adv.Eng. Mater*., 7 (2003) 563.
17. H. Zenner and F. Renner, *Int. J. Fatigue*, 24 (2002) 1255.
18. G.Song, Corros Sci. 49(2007)1696-1701.
19. F. Witte, N. Hort, C. Vogt, S. Cohen, K. U. Kainer, R. Willumeit and F. Feyerabend,*Curr. Opin. Solid State Mater. Sci.*, 12 (2008) 63.
20. G.Song , A.Atrens ,M.Dargusch, *Corros Sci*.,41(1999)249.
21. W. Fishbein and P. Carbone, *J Biol Chem*., 240 (1965)2407.
22. N. Nishino, J. Powers, *Biochem*., 18 (1979) 4340.
23. E. Petrillo and M. Ondetti, *Med. Res. Rev*., 2 (1982) 1.
24. M.Rockwell, M. Melden, R.Copeland, K. Hardman, C.Decicco and W. Degrado, *J. Am. Chem. Soc*., 118 (1996) 10337.
25. M.Miller, F. Malouin, R.Bergeron and G. Brittenham, Eds, (1994) pp 275.
26. W.Goa , H.Mitsuya , J.Driscoll and D. Johns , *Biochem Pharmacol*, 50(1995)274.
27. T. Gora and T.Robak, *Acta Haematol Pol*, 26(1995) 39.
28. L.Coutinho, M.Brereton, A.Santos and W.Ryder, J.Chang ,C.J. Harrison , J.Yin , T. Dekter and N. Testa , *Br J Haematol*, 93(1996) 869.
29. S.Nand , W.Stock , J.Godwin and S. Fisher, *Am J Haematol*, 52(1996) 42.
30. S.Santarossa, E.Vaccher, D.Lenerdon , A.Marlo, D.Errante and U.Tirelli, Eur *J.Cancer* 31A(1995)959.
31. Krakoff, N.Brown and P.Reichard, *Cancer Res*., 28 (1968)1559.
32. M. Sha-Ying , S. Pang, S. Tstram and S. Brawn, ,52(2011)1.
33. A. Dessi, G. Micera, D. Sanna and L. Erre, *J. Inorg. Biochem*., 48 (1992) 279.
34. K. Ali, N. Fatima, Z.. Maqsood and S. Kazmi, *J. Iranian Chem. Soc*., 1(2004)65.
35. E.Brien, S.Le Roy, J. Levaillain, D. Fitzgerald and K. Nloan, *Inorg. Chim.Acta* .,266(1997)117.

36. D.Anina, *Am Soc Microbiol*, 43 (1999)651.
37. Vogel's Text Book of Quantitative chemical analysis, fifth ed., Longman, UK, 1989, Ch. 10, pp. 326.
38. A.Bauer, W.Kirby, C. Sherris and M. Truck, *J. Am. Clin. Path*., 45 (1966)493.
39. M.Pfaller, L. Burmeister, M. Bartlett and M.Rinaldi, *J. Clin. Microbiol*. 26(1988) 1437.
40. National Committee for Clinical Laboratory Standards (1993), Methods for dilution antimicrobial susceptibility tests for bacteria that grow aerobically, third ed., Approved standard M7- A3. NCCLS, Villanova, Pa.
41. L.Liebowitz, H.Ashbee, E.Evans, Y. Chong, N. Mallatova, M.Zaidi and D. Gibbs, *Diagn Microbiol Infect Dis*, 27 (2001) 24.
42. M. Matar, L.Ostrosky-Zeichner, V. Paetznick, E.Rodriguez, J. Rex, *Antimicrob. Agents Chemother*, 47 (2003) 1647.
43. J. Stark and H.Wallace, *Chemistry Data Book*, Murray, London, 1975, pp. 75.
44. P. Gans, A. Sabatini and A. Vacca, *J. Inorg. Chim. Acta*, 18 (1976) 237.
45. M.Shoukry, A.Shoukry, P.Khalf Allas and S. Hassan, *Int. J. Chem.Kinet*., 42 (2010) 608.
46. A.A. Ghoneim, A.M. Fekry and M.A. Ameer, *Electrochim. Acta*, 55( 2010) 6028.
47. G. Wu, Y. Fan, A.A. Atrens, C. Zhai, W. Ding, J. Appl. Electrochem. 38 (2008)251.
48. A.M. Fekry and Rabab M. El-Sherif, *Electrochim. Acta*, 54 (2009) 7280.
49. E.Patrito and V.Macagno, *J Electroanal Chem*. ,357(1994) 203.
50. M.A.Ameer , A.M.Fekry and A.A.Ghoneim, *Corros.* , 56 (2009) 587.
51. M.A.Ameer and A.M. Fekry , *Prog. Org. Coat*., 71(2011) 343.
52. H. Wang , Y. Estrin and Z. Zúberová, *Mater. Lett*., 62 (2008) 2476.
53. X. Gu, Y. Zheng, Y. Cheng, S. Zhong and T. Xi, *Biomat*. ,30 (2009) 484.
54. M. Peuster, P. Beerbaum, F.W. Bach and H. Hauser, *Cardiol. Young*, 16 (2006)107.
55. M. Jonsson, D. Persson and D. Thierry, *Corros. Sci*., 49 (2007) 1540.
56. R. Narayanan and S.K. Seshadri, *Corros. Sci*., 49 (2007) 542.
57. G. Song and S. Song, *Adv. Eng. Mater*., 9 (2007) 298.
58. C.Ying-liang, Q.Ting-wei, W.Hui-min and Z.Zhao, *Trans. Nonferrous Met. Soc.China*, 19 (2009) 517.
59. Waffa M.Hosny, S. M. El-Medani, M.Shahira and M. Shoukry, *Annali di Chimica,*, 90(2000)277.
60. E.Khairy, M. Shoukry, M. Khalil and M. Mohamed, *TransitionMet. Chem*., 21(1996) 176.
61. M.Khalil and A. Fazary, *Monatsh. Chem*., 135(2004) 1455.
62. C.Song, H.Ryu, J. Park and T.Ko, *Bull. Kor. Chem.Soc*.,20**(**1999)722.
63. N. Sari, S. Arslan, E. Logoglu and I. Sakiyan, *G.U. J. Sci*., 16 (2003) 283.
64. B.Tweedy, *Phytopathology*, 55 (1964) 910.
65. A.Koch, *Clin. Microbiol. Rev*., 16 (2003)673.